

Synthesis and Electrochemical Characterization of Cobalt(III) Mono-Hydride Complexes Containing Pendant Amines

Eric S. Wiedner,^{*‡} John A. S. Roberts,[‡] William G. Dougherty,[†] W. Scott Kassel,[†] Daniel L. DuBois,[‡]
and R. Morris Bullock^{‡*}

[‡]*Physical Sciences Division, Pacific Northwest National Laboratory,
P.O. Box 999, K2-57, Richland, Washington 99352*

[†]*Department of Chemistry, Villanova University, 800 E. Lancaster Ave., Villanova, Pennsylvania 19085*

* E-mail: eric.wiedner@pnnl.gov, morris.bullock@pnnl.gov

<i>Table of Contents</i>	<i>Page</i>
Synthesis of phosphine precursors.	S3
Figure S1. Experimental and simulated ³¹ P{ ¹ H} NMR spectra of [HCo(L2)(CH ₃ CN)] ²⁺	S4
Table S1. NMR simulation parameters.	S4
Table S2. Selected bond angles from X-Ray diffraction.	S5
Discussion of minor coordination isomers.	S6
Figure S2. Cyclic voltammograms of a 2 × 10 ⁻³ M solution of [Co ^{II} (L3)(CH ₃ CN)] ²⁺	S6
Figure S3. Cyclic voltammogram of a 2 × 10 ⁻³ M solution of [HCo ^{III} (L3)(CH ₃ CN)] ²⁺	S7
Figure S4. Plot of <i>i</i> _{pc} versus <i>v</i> ^{1/2} for varying concentrations of [HCo ^{III} (L2)(CH ₃ CN)] ²⁺	S7
Figure S5. Plot of <i>E</i> _{pc} for [HCo ^{III} (L2)(CH ₃ CN)] ²⁺ (blue trace) and [HCo ^{III} (L3)(CH ₃ CN)] ²⁺ (red trace) vs. log(<i>v</i>).	S8

Figure S6. Cyclic voltammograms of a 2×10^{-3} M solution of $[\text{HCo}^{\text{III}}(\text{L2})(\text{CH}_3\text{CN})]^{2+}$ at a scan rate of 1 V s^{-1} with no added H_2O and 0.14 M added H_2O	S8
Figure S7. Cyclic voltammograms of a 2×10^{-3} M solution of $[\text{HCo}^{\text{III}}(\text{L2})(\text{CH}_3\text{CN})]^{2+}$ at a scan rate of 10 V s^{-1} with no added H_2O and 0.14 M added H_2O	S9
Calculation of predicted electron stoichiometry for a bulk electrolysis experiment.	S9
Figure S8. Simulated cyclic voltammogram (two cycles) of $[\text{HCo}^{\text{III}}(\text{L2})(\text{CH}_3\text{CN})]^{2+}$ at 50 V s^{-1}	S10
Figure S9. Simulated cyclic voltammogram (two cycles) of $[\text{HCo}^{\text{III}}(\text{L2})(\text{CH}_3\text{CN})]^{2+}$ at 50 V s^{-1} with adjusted K_{eq}	S10
Table S3. CV simulation parameters for monometallic mechanism 1.	S11
Table S4. CV simulation parameters for monometallic mechanism 2.	S11
Table S5. CV simulation parameters for monometallic mechanism 3.	S12
Table S6. CV simulation parameters for bimetallic mechanism 1.	S12
Table S7. CV simulation parameters for bimetallic mechanism 2.	S13
Table S8. CV simulation parameters for bimetallic mechanism 3.	S13
Table S9. CV simulation parameters for bimetallic mechanism 4.	S14
Table S10. CV simulation parameters for bimetallic mechanism 5.	S14
Table S11. CV simulation parameters for bimetallic mechanism 6.	S15
Table S12. CV simulation parameters for bimetallic mechanism 7.	S15
Table S13. CV simulation parameters for bimetallic mechanism 8.	S16
Table S14. CV simulation parameters for bimetallic mechanism 9.	S16
References.	S17

Diethyl(2-(diphenylphosphino)ethyl)phosphonate. In a modification of the previously reported procedure,¹ diphenylphosphine (19.0 mL, 0.110 mol), vinyl diethylphosphonate (18.5 mL, 0.120 mol, 1.1 equiv), and AIBN (0.8 g, 0.005 mol) were combined in a 250 mL Schlenk flask. The mixture was heated in a 65 °C oil bath for 21 h, at which point ³¹P{¹H} NMR spectroscopy of an aliquot revealed complete conversion to the desired product. The oil was heated under vacuum at 100 °C for 5 h to remove volatile byproducts, leaving diethyl(2-(diphenylphosphino)ethyl)phosphonate (37.3 g, 0.106 mol, 96 %) as a colorless oil. ¹H NMR (500 MHz, CDCl₃): δ 7.43-7.38 (m, 4H, ArH), 7.37-7.30 (m, 6H, ArH), 4.05 (m, 4H, OCH₂CH₃), 2.27 (m, 2H, P(CH₂)₂P), 1.75 (m, 2H, P(CH₂)₂P), 1.29 (t, 6H, ³J_{HH} = 7.1 Hz, OCH₂CH₃). ³¹P{¹H} NMR (CDCl₃): δ 31.86 (d, 1P, ³J_{PP} = 63.0 Hz, P(O)(OEt)₂), -12.11 (d, 1P, ³J_{PP} = 63.0 Hz, PPh₂).

Diethyl(2-(diphenylphosphino)propyl)phosphonate. Diphenylphosphine (4.6 mL, 0.026 mol), allyl diethylphosphonate (4.5 mL, 0.029 mol, 1.1 equiv), and AIBN (0.7 g, 0.004 mol) were combined in a 100 mL Schlenk flask. The mixture was heated in a 65 °C oil bath for 20 h, at which point ³¹P{¹H} NMR spectroscopy of an aliquot revealed approx. an 80 % conversion to the desired product. Additional AIBN (0.4 g, 0.002 mol) was added to the mixture, which was heated in a 65 °C oil bath for an additional 20 h. The oil was heated under vacuum at 110 °C for 5 h to remove volatile byproducts, leaving diethyl(2-(diphenylphosphino)propyl)phosphonate (8.5 g, 0.024 mol, 91 %) as a colorless oil. ¹H NMR (500 MHz, CDCl₃): δ 7.44-7.39 (m, 4H, ArH), 7.35-7.30 (m, 6H, ArH), 4.04 (m, 4H, OCH₂CH₃), 2.15 (m, 2H, P(CH₂)₃P), 1.88 (m, 2H, P(CH₂)₃P), 1.77 (m, 2H, P(CH₂)₃P), 1.27 (t, 6H, ³J_{HH} = 7.1 Hz, OCH₂CH₃). ³¹P{¹H} NMR (CDCl₃): δ 31.87 (s, 1P, P(O)(OEt)₂), -16.72 (s, 1P, PPh₂).

Diphenyl(2-phosphinoethyl)phosphine. In a modification of the previously reported procedure,¹ solid LiAlH₄ (3.2 g, 0.084 mol, 2.9 equiv) was added in portions to a solution of trimethylsilylchloride (10.0 mL, 0.079 mol, 2.7 equiv) in THF (150 mL) at -35 °C in a 250 mL Schlenk flask. The mixture was stirred at ambient temperature for 1.5 h, then the flask was cooled to -78 °C. A solution of diethyl(2-(diphenylphosphino)ethyl)phosphonate (10.2 g, 0.0291 mol) in THF (50 mL) was added slowly via cannula to the stirring reaction mixture, which was then allowed to warm to ambient temperature. After stirring for 21 h, the flask was cooled in an ice bath, then the reaction was quenched sequentially with degassed water (3 mL), 15 % (w/w) aqueous NaOH (3 mL), and degassed water (6 mL). The precipitated salts were broken up and the mixture was filtered through an inline filtration tube. The solid salts were rinsed with THF (5 × 20 mL). The filtrate was concentrated to dryness under vacuum to

afford diphenyl(2-phosphinoethyl)phosphine (6.09 g, 0.0247 mol, 85 %) as a viscous oil that solidified over the course of several days. The ^1H and $^{31}\text{P}\{^1\text{H}\}$ NMR spectra matched the literature values.¹

Diphenyl(3-phosphinopropyl)phosphine. This compound was prepared in a manner analogous to that described for diphenyl(2-phosphinoethyl)phosphine and was isolated as a viscous oil in 86 % yield. The ^1H and $^{31}\text{P}\{^1\text{H}\}$ NMR spectra matched the literature values.²

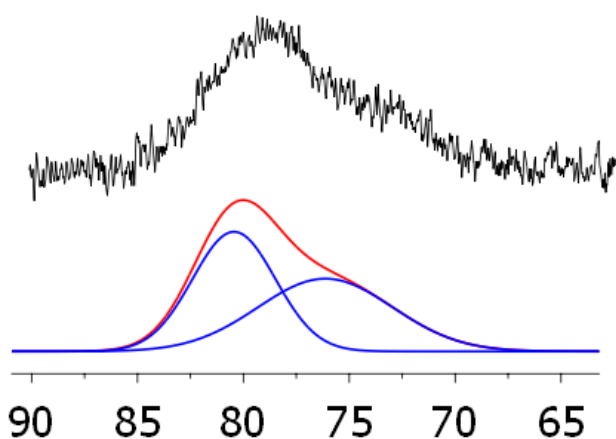


Figure S1. Experimental (top) and simulated (bottom) $^{31}\text{P}\{^1\text{H}\}$ NMR spectrum of $[\text{HCo}(\text{L2})(\text{CH}_3\text{CN})]^{2+}$. The simulated spectrum shows individual peaks (blue) and the sum peak (red).

Table S1. NMR simulation parameters.

Complex	Nucleus	Peak	δ	Height	$\Delta\nu$ (Hz)	L/G	Area
$[\text{HCo}^{\text{III}}(\text{L2})(\text{CH}_3\text{CN})]^{2+}$ Residual Error = 9.35×10^{-5}	$^{31}\text{P}\{^1\text{H}\}$	1	80.334	0.10	1035.9	0.00	492.631
		2	76.079	0.06	1682.5	0.00	499.758

Table S2. Selected bond angles (deg) from X-Ray diffraction.

$[\text{Co}^{\text{II}}(\text{L2})(\text{CH}_3\text{CN})]^{2+}$					
P(1)-Co(1)-P(2)	84.906(14)	P(1)-Co(1)-P(3)	163.470(14)	N(3)-Co(1)-P(3)	96.55(3)
P(2)-Co(1)-P(3)	81.096(14)	P(2)-Co(1)-P(4)	164.717(14)	N(3)-Co(1)-P(4)	94.21(3)
P(3)-Co(1)-P(4)	86.853(14)	N(3)-Co(1)-P(1)	93.71(3)	$\alpha(1)$	15.1
P(1)-Co(1)-P(4)	105.315(14)	N(3)-Co(1)-P(2)	96.46(3)	$\alpha(2)$	13.8
$[\text{Co}^{\text{II}}(\text{L3})(\text{CH}_3\text{CN})]^{2+}$					
P(1)-Co(1)-P(2)	90.641(15)	P(1)-Co(1)-P(3)	169.916(16)	N(3)-Co(1)-P(3)	92.70(4)
P(2)-Co(1)-P(3)	79.627(15)	P(2)-Co(1)-P(4)	162.642(16)	N(3)-Co(1)-P(4)	95.79(4)
P(3)-Co(1)-P(4)	90.639(16)	N(3)-Co(1)-P(1)	91.42(4)	$\alpha(1)$	15.2
P(1)-Co(1)-P(4)	98.102(16)	N(3)-Co(1)-P(2)	98.97(4)	$\alpha(2)$	15.2
$[\text{HCo}^{\text{III}}(\text{L2})(\text{CH}_3\text{CN})]^{2+}$					
P(1)-Co(1)-P(2)	87.273(16)	N(3)-Co(1)-P(1)	92.84(4)	H(1b)-Co(1)-P(3)	83.5(9)
P(2)-Co(1)-P(3)	80.569(16)	N(3)-Co(1)-P(2)	94.78(4)	H(1b)-Co(1)-P(4)	90.2(10)
P(3)-Co(1)-P(4)	85.327(16)	N(3)-Co(1)-P(3)	98.28(4)	H(1b)-Co(1)-N(3)	177.9(10)
P(1)-Co(1)-P(4)	105.892(16)	N(3)-Co(1)-P(4)	90.86(4)	$\alpha(1)$	12.3
P(1)-Co(1)-P(3)	164.126(18)	H(1b)-Co(1)-P(1)	85.2(9)	$\alpha(2)$	11.4
P(2)-Co(1)-P(4)	165.423(17)	H(1b)-Co(1)-P(2)	84.6(10)		
$[\text{HCo}^{\text{III}}(\text{L3})(\text{CH}_3\text{CN})]^{2+}$					
P(1)-Co(1)-P(2)	90.917(13)	N(3)-Co(1)-P(1)	96.12(3)	H(1c)-Co(1)-P(3)	77.2(8)
P(2)-Co(1)-P(3)	79.512(13)	N(3)-Co(1)-P(2)	91.83(3)	H(1c)-Co(1)-P(4)	87.7(8)
P(3)-Co(1)-P(4)	89.085(13)	N(3)-Co(1)-P(3)	102.53(3)	H(1c)-Co(1)-N(3)	176.8(8)
P(1)-Co(1)-P(4)	100.383(13)	N(3)-Co(1)-P(4)	89.13(3)	$\alpha(1)$	18.6
P(1)-Co(1)-P(3)	159.223(14)	H(1c)-Co(1)-P(1)	84.7(8)	$\alpha(2)$	18.3
P(2)-Co(1)-P(4)	168.494(13)	H(1c)-Co(1)-P(2)	91.3(8)		

$\alpha(1)$: P(2)-Co(1)-P(3) plane vs P(1)-Co(1)-P(4) plane. $\alpha(2)$: P(1)Co(1)-P(2) plane vs P(3)-Co(1)-P(4) plane

A reversible reduction wave with a half-wave potential of -1.06 V is frequently observed in cyclic voltammograms of $[\text{Co}^{\text{II}}(\text{L3})(\text{CH}_3\text{CN})]^{2+}$ and typically accounts for 5-10% of the total cobalt current intensity. The intensity of this wave can be diminished to ca. 2% of the total cobalt current intensity by performing a slow addition of $[\text{Co}^{\text{II}}(\text{CH}_3\text{CN})_6]^{2+}$ to L3 during the synthesis of $[\text{Co}^{\text{II}}(\text{L3})(\text{CH}_3\text{CN})]^{2+}$ as described in the Experimental Section. A similar reduction wave is occasionally observed in voltammograms of $[\text{Co}^{\text{II}}(\text{L2})(\text{CH}_3\text{CN})]^{2+}$, but its intensity and frequency of appearance is much less than observed for $[\text{Co}^{\text{II}}(\text{L3})(\text{CH}_3\text{CN})]^{2+}$. These reduction waves are attributed to minor coordination isomers than are formed during the syntheses of $[\text{Co}^{\text{II}}(\text{L2})(\text{CH}_3\text{CN})]^{2+}$ and $[\text{Co}^{\text{II}}(\text{L3})(\text{CH}_3\text{CN})]^{2+}$. Two possible identities for the isomers are $[\text{Co}^{\text{II}}(\text{L2/L3})_2(\text{CH}_3\text{CN})]^{2+}$ in which each L2/L3 ligand is coordinated in a bidentate fashion, or a species in which the L2/L3 ligand bridges between two cobalt atoms. The formation of these byproducts can be sufficiently minimized to prevent their interference in subsequent chemical measurements. Similar reduction waves corresponding to a trace amount of a minor impurity can also be observed in voltammograms of $[\text{HCo}^{\text{III}}(\text{L2})(\text{CH}_3\text{CN})]^{2+}$ and $[\text{HCo}^{\text{III}}(\text{L3})(\text{CH}_3\text{CN})]^{2+}$.

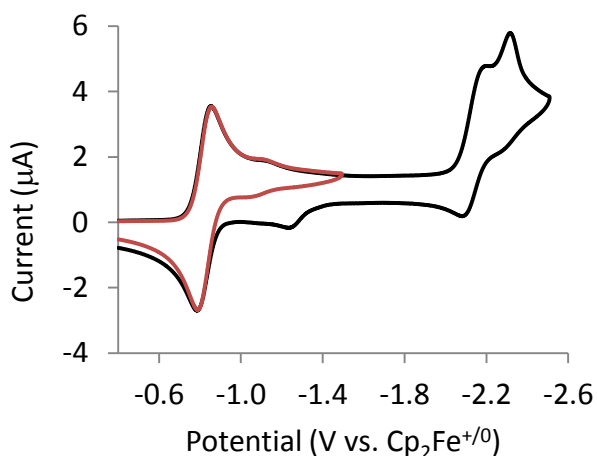


Figure S2. Cyclic voltammograms of a 2×10^{-3} M solution of $[\text{Co}^{\text{II}}(\text{L3})(\text{CH}_3\text{CN})]^{2+}$. Conditions: scan rate = 0.1 V s^{-1} , $0.2 \text{ M NBu}_4\text{PF}_6$ acetonitrile solution, glassy carbon working electrode.

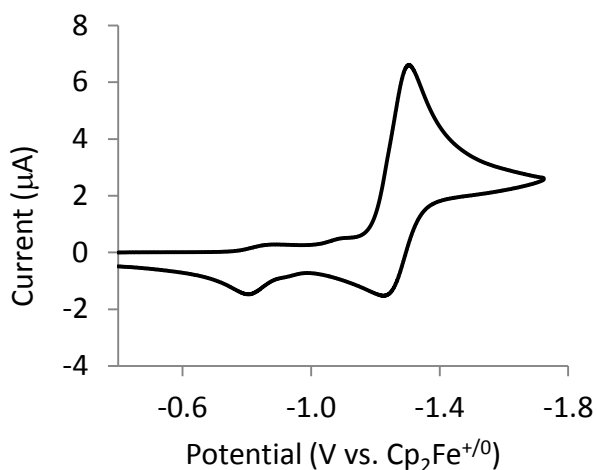


Figure S3. Cyclic voltammogram of a 2×10^{-3} M solution of $[\text{HCo}^{\text{III}}(\text{L3})(\text{CH}_3\text{CN})]^{2+}$. Conditions: scan rate = 0.1 V s^{-1} , $0.2 \text{ M NBU}_4\text{PF}_6$ acetonitrile solution, glassy carbon working electrode.

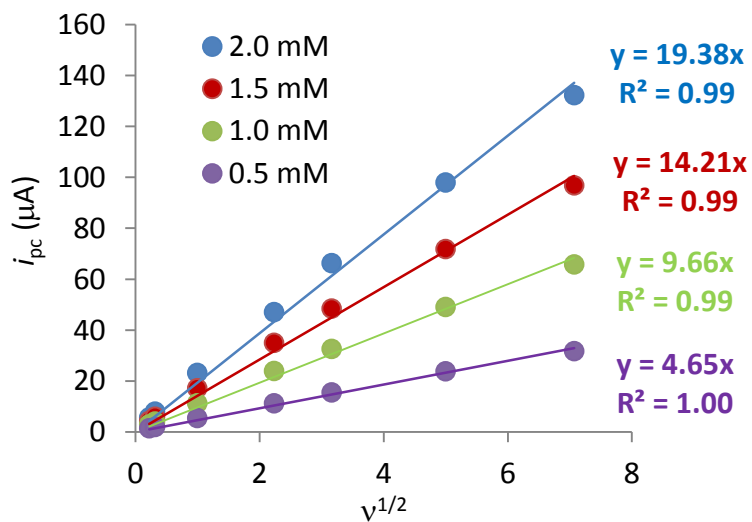


Figure S4. Plot of i_{pc} versus $v^{1/2}$ for varying concentrations of $[\text{HCo}^{\text{III}}(\text{L2})(\text{CH}_3\text{CN})]^{2+}$. Conditions: $0.2 \text{ M NBU}_4\text{PF}_6$ acetonitrile solution, glassy carbon working electrode.

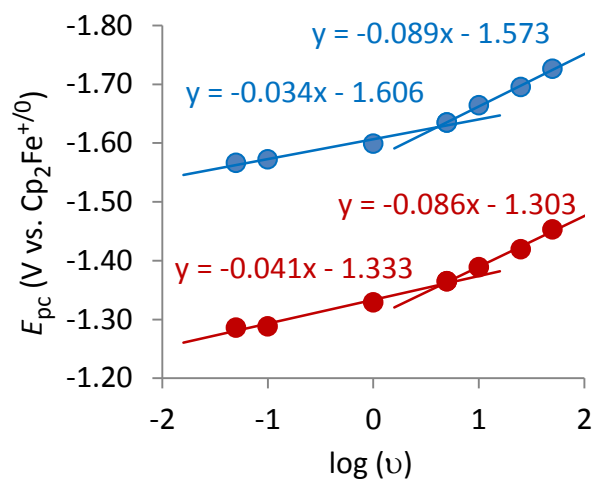


Figure S5. Plot of E_{pc} for $[\text{HCo}(\text{L2})(\text{CH}_3\text{CN})]^{2+}$ (blue trace) and $[\text{HCo}(\text{L3})(\text{CH}_3\text{CN})]^{2+}$ (red trace) vs. $\log(v)$. Conditions: 2 mM analyte, 0.2 M NBu_4PF_6 acetonitrile solution, glassy carbon working electrode.

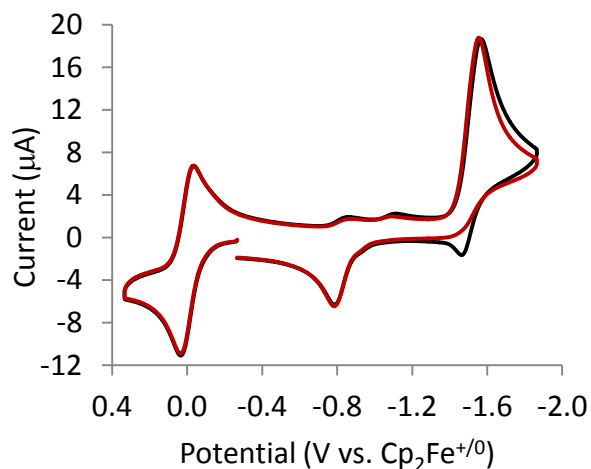


Figure S6. Cyclic voltammograms of a 2×10^{-3} M solution of $[\text{HCo}^{\text{III}}(\text{L2})(\text{CH}_3\text{CN})]^{2+}$ at a scan rate of 1 V s^{-1} with no added H_2O (black trace) and 0.14 M added H_2O (red trace). Conditions: 0.2 M NBu_4PF_6 acetonitrile solution, glassy carbon working electrode.

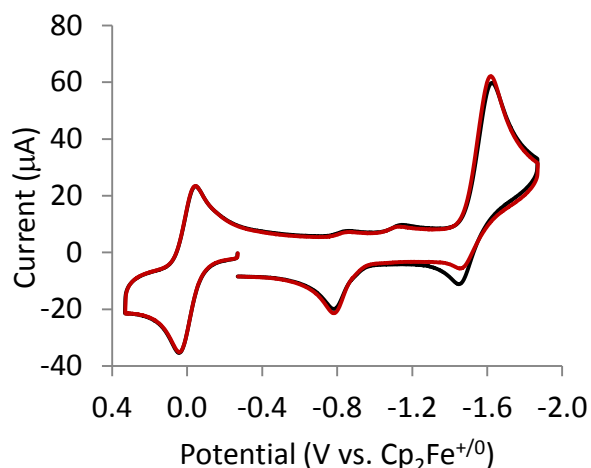


Figure S7. Cyclic voltammograms of a 2×10^{-3} M solution of $[\text{HCo}^{\text{III}}(\text{L2})(\text{CH}_3\text{CN})]^{2+}$ at a scan rate of 10 V s^{-1} with no added H_2O (black trace) and 0.14 M added H_2O (red trace). Conditions: 0.2 M NBu_4PF_6 acetonitrile solution, glassy carbon working electrode.

It has been suggested that the excess of 0.1 electrons passed in the bulk electrolysis of $[\text{HCo}^{\text{III}}(\text{L2})(\text{CH}_3\text{CN})]^{2+}$ results from consumption of trace water in a monometallic reaction ($2 e^-$ per Co) prior to bimetallic H_2 formation ($1 e^-$ per Co). The validity of this argument can be tested through a calculation of the electron stoichiometry for the bulk electrolysis performed with $[\text{HCo}^{\text{III}}] = 2.0 \text{ mM}$ and $[\text{H}_2\text{O}]$ estimated at 0.4 mM (10 ppm).

Monometallic pathway: $[\text{HCo}] = [\text{H}_2\text{O}] = 0.4 \text{ mM}$

$$0.4 \text{ mM HCo} \times (2 \text{ mM } e^- / \text{mM HCo}) = 0.8 \text{ mM } e^-$$

Bimetallic pathway: $[\text{HCo}] = [\text{HCo}^{\text{III}}] - [\text{H}_2\text{O}] = 1.6 \text{ mM}$

$$1.6 \text{ mM HCo} \times (1 \text{ mM } e^- / \text{mM HCo}) = 1.6 \text{ mM } e^-$$

Total e^- count: $(0.8 \text{ mM } e^- + 1.6 \text{ mM } e^-) / 2 \text{ mM HCo}^{\text{III}} = 1.2 e^- \text{ per Co}$

The estimated value of $1.2 e^-$ per Co is very close to the measured value of $1.1 e^-$ per Co, which supports the hypotheses that trace water is rapidly depleted in a monometallic reaction with HCo during the bulk electrolysis experiment.

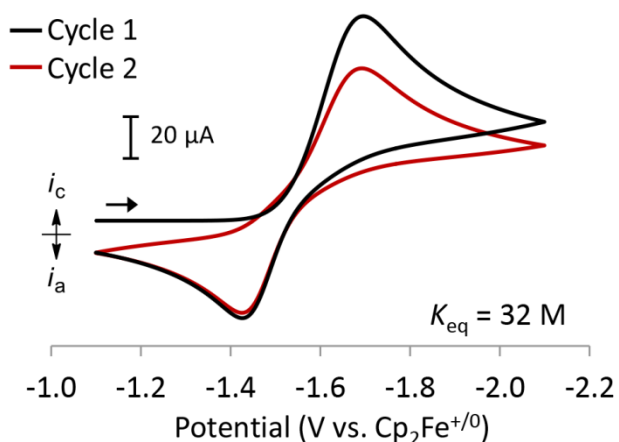


Figure S8. Simulated cyclic voltammogram (two cycles) of $[\text{HCo}^{\text{III}}(\text{L2})(\text{CH}_3\text{CN})]^{2+}$ at 50 V s^{-1} . The optimized refinement parameters from Table 2 (main text) were employed.

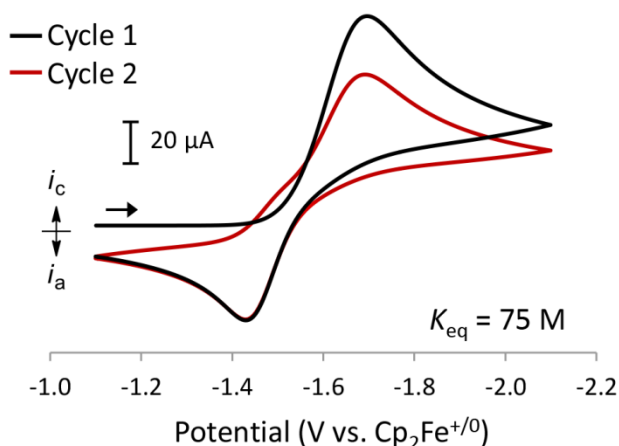


Figure S9. Simulated cyclic voltammogram (two cycles) of $[\text{HCo}^{\text{III}}(\text{L2})(\text{CH}_3\text{CN})]^{2+}$ at 50 V s^{-1} with adjusted K_{eq} . The optimized refinement parameters from Table 2 (main text) were employed, with the exception of K_{eq} for reversible acetonitrile dissociation from $[\text{HCo}^{\text{II}}(\text{L2})(\text{CH}_3\text{CN})]^+$ which was manually set to 75 M.

Table S3. CV simulation parameters for Monometallic Mechanism 1.

Monometallic Mechanism 1: $[\text{HCo}^{\text{II}}(\text{L2})(\text{CH}_3\text{CN})]^+ \rightarrow [\text{Co}^{\text{II}}(\text{L2})(\text{CH}_3\text{CN})]^{2+} + \text{H}^-$ ^a			
E° of Electron Transfer Reactions (V vs $\text{Cp}_2\text{Fe}^{+/0}$) ^b			
Conc.	$[\text{HCo}^{\text{III/II}}(\text{L2})(\text{CH}_3\text{CN})]^{2+/+}$	$[\text{HCo}^{\text{II/I}}(\text{L2})]^{+/0}$	$[\text{Co}^{\text{III/I}}(\text{L2})(\text{CH}_3\text{CN})]^{2+/+}$
2 mM	-1.5962(6)	-1.473(1)	-0.82
1 mM	-1.5863(7)	-1.472(2)	-0.82
1 mM ^c	-1.5909(6)	-1.475(1)	-0.82

Chemical Reactions and Parameters				
$[\text{HCo}^{\text{II}}(\text{L2})(\text{CH}_3\text{CN})]^+ \rightleftharpoons [\text{HCo}^{\text{II}}(\text{L2})]^+ + \text{CH}_3\text{CN}$				
Conc.	K_{eq} (M)	k_{fwd} (s^{-1})	k_{rev} ($\text{M}^{-1}\text{s}^{-1}$) ^d	k_{fwd} (s^{-1}) ^e
2 mM	38(4)	$9.7(3) \times 10^2$	25	136(6)
1 mM	20(3)	$6.6(3) \times 10^2$	30	99(4)
1 mM ^c	38	9.7×10^2	25	138(4)

^a Uncertainties are given at the 2σ (95.4%) confidence level and are generated in the least-squares refinement. ^b Butler-Volmer transfer coefficient (α) was fixed at 0.5 and heterogeneous electron transfer rate constant (k°) was fixed at 0.1 cm s^{-1} for all electron transfer reactions. ^c K_{eq} and k_{fwd} for reversible acetonitrile dissociation from $[\text{HCo}^{\text{II}}(\text{L2})(\text{CH}_3\text{CN})]^+$ were fixed to the optimized values obtained from refinement on the 2 mM analyte data set. ^d $k_{\text{rev}} = k_{\text{fwd}}/K_{\text{eq}}$.

Table S4. CV simulation parameters for Monometallic Mechanism 2.

Monometallic Mechanism 2: $[\text{HCo}^{\text{II}}(\text{L2})]^+ \rightarrow [\text{Co}^{\text{II}}(\text{L2})(\text{CH}_3\text{CN})]^{2+} + \text{H}^-$ ^a			
E° of Electron Transfer Reactions (V vs $\text{Cp}_2\text{Fe}^{+/0}$) ^b			
Conc.	$[\text{HCo}^{\text{III/II}}(\text{L2})(\text{CH}_3\text{CN})]^{2+/+}$	$[\text{HCo}^{\text{II/I}}(\text{L2})]^{+/0}$	$[\text{Co}^{\text{III/I}}(\text{L2})(\text{CH}_3\text{CN})]^{2+/+}$
2 mM	-1.595 ^c	-1.470 ^c	-0.82
1 mM	-1.595 ^c	-1.470 ^c	-0.82
1 mM ^d	-1.5919(9)	-1.474(2)	-0.82

Chemical Reactions and Parameters				
$[\text{HCo}^{\text{II}}(\text{L2})(\text{CH}_3\text{CN})]^+ \rightleftharpoons [\text{HCo}^{\text{II}}(\text{L2})]^+ + \text{CH}_3\text{CN}$				
Conc.	K_{eq} (M)	k_{fwd} (s^{-1})	k_{rev} ($\text{M}^{-1}\text{s}^{-1}$) ^e	k_{fwd} (s^{-1}) ^e
2 mM	38(5)	1.065×10^3 ^c	28	78(9)
1 mM	23(4)	$7.8(4) \times 10^2$	35	117(8)
1 mM ^d	38	1.065×10^3	28	152(8)

^a Uncertainties are given at the 2σ (95.4%) confidence level and are generated in the least-squares refinement. ^b Butler-Volmer transfer coefficient (α) was fixed at 0.5 and heterogeneous electron transfer rate constant (k°) was fixed at 0.1 cm s^{-1} for all electron transfer reactions. ^c Value was fixed manually in order for the refinement to converge. ^d K_{eq} and k_{fwd} for reversible acetonitrile dissociation from $[\text{HCo}^{\text{II}}(\text{L2})(\text{CH}_3\text{CN})]^+$ were fixed to the optimized values obtained from refinement on the 2 mM analyte data set. ^e $k_{\text{rev}} = k_{\text{fwd}}/K_{\text{eq}}$.

Table S5. CV simulation parameters for Monometallic Mechanism 3.

Monometallic Mechanism 3: $[\text{HCo}^{\text{I}}(\text{L2})]^+ \rightarrow [\text{Co}^{\text{I}}(\text{L2})(\text{CH}_3\text{CN})]^+ + \text{H}^-$ ^a			
E° of Electron Transfer Reactions (V vs $\text{Cp}_2\text{Fe}^{+/0}$) ^b			
Conc.	$[\text{HCo}^{\text{III/II}}(\text{L2})(\text{CH}_3\text{CN})]^{2+/+}$	$[\text{HCo}^{\text{II/I}}(\text{L2})]^{+/0}$	$[\text{Co}^{\text{III/I}}(\text{L2})(\text{CH}_3\text{CN})]^{2+/+}$
2 mM	-1.5960(6)	-1.478(1)	-0.82
1 mM	-1.5860(7)	-1.478(2)	-0.82
1 mM ^c	-1.5907(6)	-1.478(1)	-0.82

Chemical Reactions and Parameters				
$[\text{HCo}^{\text{II}}(\text{L2})(\text{CH}_3\text{CN})]^+ \rightleftharpoons [\text{HCo}^{\text{I}}(\text{L2})]^+ \rightarrow [\text{Co}^{\text{I}}(\text{L2})(\text{CH}_3\text{CN})]^+ + \text{H}^-$				
Conc.	K_{eq} (M)	k_{fwd} (s^{-1})	k_{rev} ($\text{M}^{-1}\text{s}^{-1}$) ^d	k_{fwd} (s^{-1})
2 mM	112(7)	$1.00(4) \times 10^3$	9	1.94(8)
1 mM	64(4)	$6.5(2) \times 10^2$	10	2.3(1)
1 mM ^c	112	1.00×10^3	9	2.07(9)

^a Uncertainties are given at the 2σ (95.4%) confidence level and are generated in the least-squares refinement. ^b Butler-Volmer transfer coefficient (α) was fixed at 0.5 and heterogeneous electron transfer rate constant (k°) was fixed at 0.1 cm s^{-1} for all electron transfer reactions. ^c K_{eq} and k_{fwd} for reversible acetonitrile dissociation from $[\text{HCo}^{\text{II}}(\text{L2})(\text{CH}_3\text{CN})]^+$ were fixed to the optimized values obtained from refinement on the 2 mM analyte data set. ^d $k_{\text{rev}} = k_{\text{fwd}}/K_{\text{eq}}$.

Table S6. CV simulation parameters for Bimetallic Mechanism 1.

Bimetallic Mechanism 1: $[\text{HCo}^{\text{III}}(\text{L2})(\text{CH}_3\text{CN})]^{2+} + [\text{HCo}^{\text{II}}(\text{L2})(\text{CH}_3\text{CN})]^+ \rightarrow [\text{Co}^{\text{II}}(\text{L2})(\text{CH}_3\text{CN})]^{2+} + [\text{Co}^{\text{I}}(\text{L2})(\text{CH}_3\text{CN})]^+ + 1/2 \text{H}_2$ ^a			
E° of Electron Transfer Reactions (V vs $\text{Cp}_2\text{Fe}^{+/0}$) ^b			
Conc.	$[\text{HCo}^{\text{III/II}}(\text{L2})(\text{CH}_3\text{CN})]^{2+/+}$	$[\text{HCo}^{\text{II/I}}(\text{L2})]^{+/0}$	$[\text{Co}^{\text{III/I}}(\text{L2})(\text{CH}_3\text{CN})]^{2+/+}$
2 mM	-1.6082(7)	-1.4732(9)	-0.82
1 mM	-1.5997(8)	-1.473(1)	-0.82
1 mM ^c	-1.6037(5)	-1.475(1)	-0.82

Chemical Reactions and Parameters				
$[\text{HCo}^{\text{II}}(\text{L2})(\text{CH}_3\text{CN})]^+ \rightleftharpoons [\text{HCo}^{\text{III}}(\text{L2})(\text{CH}_3\text{CN})]^{2+} + [\text{HCo}^{\text{II}}(\text{L2})(\text{CH}_3\text{CN})]^+ \rightarrow [\text{Co}^{\text{II}}(\text{L2})(\text{CH}_3\text{CN})]^{2+} + [\text{Co}^{\text{I}}(\text{L2})(\text{CH}_3\text{CN})]^+ + 1/2 \text{H}_2$				
Conc.	K_{eq} (M)	k_{fwd} (s^{-1})	k_{rev} ($\text{M}^{-1}\text{s}^{-1}$) ^d	k_{fwd} ($\text{M}^{-1}\text{s}^{-1}$)
2 mM	125(8)	$2.1(1) \times 10^3$	17	$3.0(2) \times 10^5$
1 mM	60(4)	$1.48(8) \times 10^3$	24	$5.3(4) \times 10^5$
1 mM ^c	125	2.1×10^3	17	$5.3(4) \times 10^5$

^a Uncertainties are given at the 2σ (95.4%) confidence level and are generated in the least-squares refinement. ^b Butler-Volmer transfer coefficient (α) was fixed at 0.5 and heterogeneous electron transfer rate constant (k°) was fixed at 0.1 cm s^{-1} for all electron transfer reactions. ^c K_{eq} and k_{fwd} for reversible acetonitrile dissociation from $[\text{HCo}^{\text{II}}(\text{L2})(\text{CH}_3\text{CN})]^+$ were fixed to the optimized values obtained from refinement on the 2 mM analyte data set. ^d $k_{\text{rev}} = k_{\text{fwd}}/K_{\text{eq}}$.

Table S7. CV simulation parameters for Bimetallic Mechanism 2.

Bimetallic Mechanism 2: $[\text{HCo}^{\text{III}}(\text{L2})(\text{CH}_3\text{CN})]^{2+} + [\text{HCo}^{\text{II}}(\text{L2})]^+ \rightarrow [\text{Co}^{\text{II}}(\text{L2})(\text{CH}_3\text{CN})]^{2+} + [\text{Co}^{\text{I}}(\text{L2})(\text{CH}_3\text{CN})]^+ + 1/2 \text{H}_2$ ^a				
<i>E</i>^o of Electron Transfer Reactions (V vs $\text{Cp}_2\text{Fe}^{+/0}$)^b				
Conc.	$[\text{HCo}^{\text{III/II}}(\text{L2})(\text{CH}_3\text{CN})]^{2+/+}$	$[\text{HCo}^{\text{II/I}}(\text{L2})]^{+/0}$	$[\text{Co}^{\text{III/I}}(\text{L2})(\text{CH}_3\text{CN})]^{2+/+}$	
2 mM	-1.5995(6)	-1.4723(9)	-0.82	
1 mM	-1.5912(6)	-1.471(1)	-0.82	
1 mM ^c	-1.5941(5)	-1.474(1)	-0.82	
Chemical Reactions and Parameters				
Conc.	K_{eq} (M)	$[\text{HCo}^{\text{II}}(\text{L2})(\text{CH}_3\text{CN})]^+ \rightleftharpoons [\text{HCo}^{\text{II}}(\text{L2})]^+ + \text{CH}_3\text{CN}$		$[\text{HCo}^{\text{III}}(\text{L2})(\text{CH}_3\text{CN})]^{2+} + [\text{HCo}^{\text{II}}(\text{L2})]^+ \rightarrow$
		k_{fwd} (s ⁻¹)	k_{rev} (M ⁻¹ s ⁻¹) ^d	$[\text{Co}^{\text{II}}(\text{L2})(\text{CH}_3\text{CN})]^{2+} + [\text{Co}^{\text{I}}(\text{L2})(\text{CH}_3\text{CN})]^+ + 1/2 \text{H}_2$
2 mM	78(5)	$1.18(4) \times 10^3$	15	$4.3(3) \times 10^4$
1 mM	39(3)	$8.9(3) \times 10^2$	23	$1.49(9) \times 10^5$
1 mM ^c	78	1.18×10^3	15	$1.17(4) \times 10^5$

^a Uncertainties are given at the 2σ (95.4%) confidence level and are generated in the least-squares refinement. ^b Butler-Volmer transfer coefficient (α) was fixed at 0.5 and heterogeneous electron transfer rate constant (*k*^o) was fixed at 0.1 cm s⁻¹ for all electron transfer reactions. ^c *K*_{eq} and *k*_{fwd} for reversible acetonitrile dissociation from $[\text{HCo}^{\text{II}}(\text{L2})(\text{CH}_3\text{CN})]^+$ were fixed to the optimized values obtained from refinement on the 2 mM analyte data set. ^d *k*_{rev} = *k*_{fwd}/*K*_{eq}.

Table S8. CV simulation parameters for Bimetallic Mechanism 3.

Bimetallic Mechanism 3: $[\text{HCo}^{\text{III}}(\text{L2})(\text{CH}_3\text{CN})]^{2+} + \text{HCo}^{\text{I}}(\text{L2}) \rightarrow [\text{Co}^{\text{II}}(\text{L2})(\text{CH}_3\text{CN})]^{2+} + \text{Co}^0(\text{L2}) + 1/2 \text{H}_2$ ^a				
<i>E</i>^o of Electron Transfer Reactions (V vs $\text{Cp}_2\text{Fe}^{+/0}$)^b				
Conc.	$[\text{HCo}^{\text{III/II}}(\text{L2})(\text{CH}_3\text{CN})]^{2+/+}$	$[\text{HCo}^{\text{II/I}}(\text{L2})]^{+/0}$	$[\text{Co}^{\text{II/I}}(\text{L2})(\text{CH}_3\text{CN})]^{2+}$ II/I, I/0	
2 mM	-1.5974(6)	-1.477(1)	-0.82, -2.52	
1 mM	-1.5877(7)	-1.478(2)	-0.82, -2.52	
1 mM ^c	-1.5923(6)	-1.479(1)	-0.82, -2.52	
Chemical Reactions and Parameters				
Conc.	K_{eq} (M)	$[\text{HCo}^{\text{II}}(\text{L2})(\text{CH}_3\text{CN})]^+ \rightleftharpoons [\text{HCo}^{\text{II}}(\text{L2})]^+ + \text{CH}_3\text{CN}$		$[\text{HCo}^{\text{III}}(\text{L2})(\text{CH}_3\text{CN})]^{2+} + \text{HCo}^{\text{I}}(\text{L2}) \rightarrow$
		k_{fwd} (s ⁻¹)	k_{rev} (M ⁻¹ s ⁻¹) ^d	$[\text{Co}^{\text{II}}(\text{L2})(\text{CH}_3\text{CN})]^{2+} + \text{Co}^0(\text{L2}) + 1/2 \text{H}_2$
2 mM	135(8)	$1.03(4) \times 10^3$	8	$2.05(9) \times 10^3$
1 mM	70(5)	$6.7(2) \times 10^2$	10	$6.0(3) \times 10^3$
1 mM ^c	135	1.03×10^3	8	$5.2(3) \times 10^3$

^a Uncertainties are given at the 2σ (95.4%) confidence level and are generated in the least-squares refinement. ^b Butler-Volmer transfer coefficient (α) was fixed at 0.5 and heterogeneous electron transfer rate constant (*k*^o) was fixed at 0.1 cm s⁻¹ for all electron transfer reactions. ^c *K*_{eq} and *k*_{fwd} for reversible acetonitrile dissociation from $[\text{HCo}^{\text{II}}(\text{L2})(\text{CH}_3\text{CN})]^+$ were fixed to the optimized values obtained from refinement on the 2 mM analyte data set. ^d *k*_{rev} = *k*_{fwd}/*K*_{eq}.

Table S9. CV simulation parameters for Bimetallic Mechanism 4.

Bimetallic Mechanism 4: $[\text{HCo}^{\text{II}}(\text{L2})(\text{CH}_3\text{CN})]^+ + [\text{HCo}^{\text{II}}(\text{L2})(\text{CH}_3\text{CN})]^+ \rightarrow$ $[\text{Co}^{\text{I}}(\text{L2})(\text{CH}_3\text{CN})]^+ + [\text{Co}^{\text{I}}(\text{L2})(\text{CH}_3\text{CN})]^+ + 1/2 \text{H}_2^a$				
E° of Electron Transfer Reactions (V vs $\text{Cp}_2\text{Fe}^{+/0}$) ^b				
Conc.	$[\text{HCo}^{\text{III/II}}(\text{L2})(\text{CH}_3\text{CN})]^{2+/+}$	$[\text{HCo}^{\text{II/I}}(\text{L2})]^{+/0}$	$[\text{Co}^{\text{II/I}}(\text{L2})(\text{CH}_3\text{CN})]^{2+/+}$	
2 mM	-1.595 ^c	-1.475 ^c		-0.82
1 mM	-1.595 ^c	-1.475 ^c		-0.82
1 mM ^d	-1.595 ^c	-1.475 ^c		-0.82
Chemical Reactions and Parameters				
$[\text{HCo}^{\text{II}}(\text{L2})(\text{CH}_3\text{CN})]^+ \rightleftharpoons [\text{HCo}^{\text{II}}(\text{L2})(\text{CH}_3\text{CN})]^+ + [\text{HCo}^{\text{II}}(\text{L2})(\text{CH}_3\text{CN})]^+ \rightarrow$ $[\text{HCo}^{\text{II}}(\text{L2})]^+ + \text{CH}_3\text{CN} \quad [\text{Co}^{\text{I}}(\text{L2})(\text{CH}_3\text{CN})]^+ + [\text{Co}^{\text{I}}(\text{L2})(\text{CH}_3\text{CN})]^+ + 1/2 \text{H}_2$				
Conc.	K_{eq} (M)	k_{fwd} (s ⁻¹)	k_{rev} (M ⁻¹ s ⁻¹) ^e	k_{fwd} (M ⁻¹ s ⁻¹)
2 mM	235(15)	$1.29(5) \times 10^3$	6	$4.8(5) \times 10^5$
1 mM	90(7)	$2.3(1) \times 10^3$	25	$6.1(6) \times 10^6$
1 mM ^d	235	1.29×10^3	6	$2.2(1) \times 10^6$

^a Uncertainties are given at the 2σ (95.4%) confidence level and are generated in the least-squares refinement. ^b Butler-Volmer transfer coefficient (α) was fixed at 0.5 and heterogeneous electron transfer rate constant (k°) was fixed at 0.1 cm s⁻¹ for all electron transfer reactions. ^c Value was fixed manually in order for the refinement to converge. ^d K_{eq} and k_{fwd} for reversible acetonitrile dissociation from $[\text{HCo}^{\text{II}}(\text{L2})(\text{CH}_3\text{CN})]^+$ were fixed to the optimized values obtained from refinement on the 2 mM analyte data set. ^e $k_{\text{rev}} = k_{\text{fwd}}/K_{\text{eq}}$.

Table S10. CV simulation parameters for Bimetallic Mechanism 5.

Bimetallic Mechanism 5: $[\text{HCo}^{\text{II}}(\text{L2})(\text{CH}_3\text{CN})]^+ + [\text{HCo}^{\text{II}}(\text{L2})]^+ \rightarrow [\text{Co}^{\text{I}}(\text{L2})(\text{CH}_3\text{CN})]^+$ $+ [\text{Co}^{\text{I}}(\text{L2})(\text{CH}_3\text{CN})]^+ + 1/2 \text{H}_2^a$				
E° of Electron Transfer Reactions (V vs $\text{Cp}_2\text{Fe}^{+/0}$) ^b				
Conc.	$[\text{HCo}^{\text{III/II}}(\text{L2})(\text{CH}_3\text{CN})]^{2+/+}$	$[\text{HCo}^{\text{II/I}}(\text{L2})]^{+/0}$	$[\text{Co}^{\text{II/I}}(\text{L2})(\text{CH}_3\text{CN})]^{2+/+}$	
2 mM	-1.595 ^c	-1.470 ^c		-0.82
1 mM	-1.595 ^c	-1.470 ^c		-0.82
1 mM ^d	-1.595 ^c	-1.470 ^c		-0.82
Chemical Reactions and Parameters				
$[\text{HCo}^{\text{II}}(\text{L2})(\text{CH}_3\text{CN})]^+ \rightleftharpoons [\text{HCo}^{\text{II}}(\text{L2})(\text{CH}_3\text{CN})]^+ + [\text{HCo}^{\text{II}}(\text{L2})]^+ \rightarrow$ $[\text{HCo}^{\text{II}}(\text{L2})]^+ + \text{CH}_3\text{CN} \quad [\text{Co}^{\text{I}}(\text{L2})(\text{CH}_3\text{CN})]^+ + [\text{Co}^{\text{I}}(\text{L2})(\text{CH}_3\text{CN})]^+ + 1/2 \text{H}_2$				
Conc.	K_{eq} (M)	k_{fwd} (s ⁻¹)	k_{rev} (M ⁻¹ s ⁻¹) ^e	k_{fwd} (M ⁻¹ s ⁻¹)
2 mM	143(9)	$1.31(5) \times 10^3$	9	$8.0(5) \times 10^5$
1 mM	90(7)	$1.51(7) \times 10^3$	17	$3.3(3) \times 10^6$
1 mM ^d	143	1.31×10^3	9	$2.5(1) \times 10^6$

^a Uncertainties are given at the 2σ (95.4%) confidence level and are generated in the least-squares refinement. ^b Butler-Volmer transfer coefficient (α) was fixed at 0.5 and heterogeneous electron transfer rate constant (k°) was fixed at 0.1 cm s⁻¹ for all electron transfer reactions. ^c Value was fixed manually in order for the refinement to converge. ^d K_{eq} and k_{fwd} for reversible acetonitrile dissociation from $[\text{HCo}^{\text{II}}(\text{L2})(\text{CH}_3\text{CN})]^+$ were fixed to the optimized values obtained from refinement on the 2 mM analyte data set. ^e $k_{\text{rev}} = k_{\text{fwd}}/K_{\text{eq}}$.

Table S11. CV simulation parameters for Bimetallic Mechanism 6.

Bimetallic Mechanism 6: $[\text{HCo}^{\text{II}}(\text{L2})(\text{CH}_3\text{CN})]^+ + \text{HCo}^{\text{I}}(\text{L2}) \rightarrow [\text{Co}^{\text{I}}(\text{L2})(\text{CH}_3\text{CN})]^+ + \text{Co}^{\text{0}}(\text{L2}) + 1/2 \text{H}_2$ ^a				
<i>E</i> ^o of Electron Transfer Reactions (V vs $\text{Cp}_2\text{Fe}^{+/0}$) ^b				
Conc.	$[\text{HCo}^{\text{III/II}}(\text{L2})(\text{CH}_3\text{CN})]^{2+/+}$	$[\text{HCo}^{\text{II/I}}(\text{L2})]^{+/0}$	$[\text{Co}^{\text{II/I}}(\text{L2})(\text{CH}_3\text{CN})]^{2+}$	II/I, I/0
2 mM	-1.5994(6)	-1.476(1)		-0.82, -2.52
1 mM	-1.5929(7)	-1.476(2)		-0.82, -2.52
1 mM ^c	-1.5929(6)	-1.478(1)		-0.82, -2.52
Chemical Reactions and Parameters				
Conc.	<i>K</i> _{eq} (M)	$[\text{HCo}^{\text{II}}(\text{L2})(\text{CH}_3\text{CN})]^+ \rightleftharpoons [\text{HCo}^{\text{II}}(\text{L2})]^+ + \text{CH}_3\text{CN}$		$[\text{HCo}^{\text{III}}(\text{L2})(\text{CH}_3\text{CN})]^{2+} + \text{HCo}^{\text{I}}(\text{L2}) \rightarrow$
		<i>k</i> _{fwd} (s ⁻¹)	<i>k</i> _{rev} (M ⁻¹ s ⁻¹) ^d	$[\text{Co}^{\text{I}}(\text{L2})(\text{CH}_3\text{CN})]^+ + \text{Co}^{\text{0}}(\text{L2}) + 1/2 \text{H}_2$
2 mM	86(5)	$9.4(3) \times 10^2$	11	$9.2(4) \times 10^4$
1 mM	60(4)	$3.6(7) \times 10^3$	16	$1.6(1) \times 10^5$
1 mM ^c	86	9.4×10^2	11	$1.65(6) \times 10^5$

^a Uncertainties are given at the 2σ (95.4%) confidence level and are generated in the least-squares refinement. ^b Butler-Volmer transfer coefficient (α) was fixed at 0.5 and heterogeneous electron transfer rate constant (*k*^o) was fixed at 0.1 cm s⁻¹ for all electron transfer reactions. ^c *K*_{eq} and *k*_{fwd} for reversible acetonitrile dissociation from $[\text{HCo}^{\text{II}}(\text{L2})(\text{CH}_3\text{CN})]^+$ were fixed to the optimized values obtained from refinement on the 2 mM analyte data set. ^d *k*_{rev} = *k*_{fwd} / *K*_{eq}.

Table S12. CV simulation parameters for Bimetallic Mechanism 7.

Bimetallic Mechanism 7: $[\text{HCo}^{\text{II}}(\text{L2})]^+ + [\text{HCo}^{\text{II}}(\text{L2})]^+ \rightarrow [\text{Co}^{\text{I}}(\text{L2})(\text{CH}_3\text{CN})]^+ + [\text{Co}^{\text{I}}(\text{L2})(\text{CH}_3\text{CN})]^+ + 1/2 \text{H}_2$ ^a				
<i>E</i> ^o of Electron Transfer Reactions (V vs $\text{Cp}_2\text{Fe}^{+/0}$) ^b				
Conc.	$[\text{HCo}^{\text{III/II}}(\text{L2})(\text{CH}_3\text{CN})]^{2+/+}$	$[\text{HCo}^{\text{II/I}}(\text{L2})]^{+/0}$	$[\text{Co}^{\text{II/I}}(\text{L2})(\text{CH}_3\text{CN})]^{2+/+}$	
2 mM	-1.5997(6)	-1.4722(9)		-0.82
1 mM	-1.5911(6)	-1.472(1)		-0.82
1 mM ^c	-1.5946(5)	-1.472(1)		-0.82
Chemical Reactions and Parameters				
Conc.	<i>K</i> _{eq} (M)	$[\text{HCo}^{\text{II}}(\text{L2})(\text{CH}_3\text{CN})]^+ \rightleftharpoons [\text{HCo}^{\text{II}}(\text{L2})]^+ + \text{CH}_3\text{CN}$		$[\text{HCo}^{\text{II}}(\text{L2})]^+ + [\text{HCo}^{\text{II}}(\text{L2})]^+ \rightarrow [\text{Co}^{\text{I}}(\text{L2})(\text{CH}_3\text{CN})]^+$
		<i>k</i> _{fwd} (s ⁻¹)	<i>k</i> _{rev} (M ⁻¹ s ⁻¹) ^d	$+ [\text{Co}^{\text{I}}(\text{L2})(\text{CH}_3\text{CN})]^+ + 1/2 \text{H}_2$
2 mM	170(1)	$1.20(4) \times 10^3$	7	$2.1(2) \times 10^5$
1 mM	90(8)	$8.9(3) \times 10^2$	10	$7.7(8) \times 10^5$
1 mM ^c	170	1.20×10^3	7	$8.0(5) \times 10^5$

^a Uncertainties are given at the 2σ (95.4%) confidence level and are generated in the least-squares refinement. ^b Butler-Volmer transfer coefficient (α) was fixed at 0.5 and heterogeneous electron transfer rate constant (*k*^o) was fixed at 0.1 cm s⁻¹ for all electron transfer reactions. ^c *K*_{eq} and *k*_{fwd} for reversible acetonitrile dissociation from $[\text{HCo}^{\text{II}}(\text{L2})(\text{CH}_3\text{CN})]^+$ were fixed to the optimized values obtained from refinement on the 2 mM analyte data set. ^d *k*_{rev} = *k*_{fwd} / *K*_{eq}.

Table S13. CV simulation parameters for Bimetallic Mechanism 8.

Bimetallic Mechanism 8: $[\text{HCo}^{\text{II}}(\text{L2})]^+ + \text{HCo}^{\text{I}}(\text{L2}) \rightarrow [\text{Co}^{\text{I}}(\text{L2})(\text{CH}_3\text{CN})]^+ + \text{Co}^0(\text{L2}) + 1/2 \text{H}_2$ ^a				
E° of Electron Transfer Reactions (V vs $\text{Cp}_2\text{Fe}^{+/0}$) ^b				
Conc.	$[\text{HCo}^{\text{III/II}}(\text{L2})(\text{CH}_3\text{CN})]^{2+/+}$	$[\text{HCo}^{\text{II/I}}(\text{L2})]^{+/0}$	$[\text{Co}^{\text{II}}(\text{L2})(\text{CH}_3\text{CN})]^{2+}$	II/I, I/0
2 mM	-1.6004(6)	-1.437(1)		-0.82, -2.52
1 mM	-1.5912(7)	-1.473(1)		-0.82, -2.52
1 mM ^c	-1.5953(6)	-1.474(1)		-0.82, -2.52
Chemical Reactions and Parameters				
$[\text{HCo}^{\text{II}}(\text{L2})(\text{CH}_3\text{CN})]^+ \rightleftharpoons [\text{HCo}^{\text{II}}(\text{L2})]^+ + \text{CH}_3\text{CN}$				
$[\text{HCo}^{\text{II}}(\text{L2})]^+ + [\text{HCo}^{\text{II}}(\text{L2})]^+ \rightarrow [\text{Co}^{\text{I}}(\text{L2})(\text{CH}_3\text{CN})]^+ + \text{Co}^0(\text{L2}) + 1/2 \text{H}_2$				
Conc.	K_{eq} (M)	k_{fwd} (s^{-1})	k_{rev} ($\text{M}^{-1}\text{s}^{-1}$) ^d	k_{fwd} ($\text{M}^{-1} \text{s}^{-1}$)
2 mM	120(8)	$1.24(4) \times 10^3$	10	$4.2(2) \times 10^4$
1 mM	61(4)	$8.7(3) \times 10^2$	14	$1.18(6) \times 10^5$
1 mM ^c	120	1.24×10^3	10	$1.21(5) \times 10^5$

^a Uncertainties are given at the 2σ (95.4%) confidence level and are generated in the least-squares refinement. ^b Butler-Volmer transfer coefficient (α) was fixed at 0.5 and heterogeneous electron transfer rate constant (k°) was fixed at 0.1 cm s^{-1} for all electron transfer reactions. ^c K_{eq} and k_{fwd} for reversible acetonitrile dissociation from $[\text{HCo}^{\text{II}}(\text{L2})(\text{CH}_3\text{CN})]^+$ were fixed to the optimized values obtained from refinement on the 2 mM analyte data set. ^d $k_{\text{rev}} = k_{\text{fwd}}/K_{\text{eq}}$.

Table S14. CV simulation parameters for Bimetallic Mechanism 9.

Bimetallic Mechanism 8: $\text{HCo}^{\text{I}}(\text{L2}) + \text{HCo}^{\text{I}}(\text{L2}) \rightarrow \text{Co}^0(\text{L2}) + \text{Co}^0(\text{L2}) + 1/2 \text{H}_2$ ^a				
E° of Electron Transfer Reactions (V vs $\text{Cp}_2\text{Fe}^{+/0}$) ^b				
Conc.	$[\text{HCo}^{\text{III/II}}(\text{L2})(\text{CH}_3\text{CN})]^{2+/+}$	$[\text{HCo}^{\text{II/I}}(\text{L2})]^{+/0}$	$[\text{Co}^{\text{II}}(\text{L2})(\text{CH}_3\text{CN})]^{2+}$	II/I, I/0
2 mM	-1.5974(7)	-1.476(1)		-0.82, -2.52
1 mM	-1.5878(7)	-1.476(1)		-0.82, -2.52
1 mM ^c	-1.5919(6)	-1.478(2)		-0.82, -2.52
Chemical Reactions and Parameters				
$[\text{HCo}^{\text{II}}(\text{L2})(\text{CH}_3\text{CN})]^+ \rightleftharpoons [\text{HCo}^{\text{II}}(\text{L2})]^+ + \text{CH}_3\text{CN}$				
$\text{HCo}^{\text{I}}(\text{L2}) + \text{HCo}^{\text{I}}(\text{L2}) \rightarrow \text{Co}^0(\text{L2}) + \text{Co}^0(\text{L2}) + 1/2 \text{H}_2$				
Conc.	K_{eq} (M)	k_{fwd} (s^{-1})	k_{rev} ($\text{M}^{-1}\text{s}^{-1}$) ^d	k_{fwd} ($\text{M}^{-1} \text{s}^{-1}$)
2 mM	142(9)	$1.0(8) \times 10^3$	7	$1.06(6) \times 10^3$
1 mM	70(6)	$6.8(3) \times 10^2$	10	$3.7(2) \times 10^3$
1 mM ^c	142	1.0×10^3	7	$2.9(2) \times 10^3$

^a Uncertainties are given at the 2σ (95.4%) confidence level and are generated in the least-squares refinement. ^b Butler-Volmer transfer coefficient (α) was fixed at 0.5 and heterogeneous electron transfer rate constant (k°) was fixed at 0.1 cm s^{-1} for all electron transfer reactions. ^c K_{eq} and k_{fwd} for reversible acetonitrile dissociation from $[\text{HCo}^{\text{II}}(\text{L2})(\text{CH}_3\text{CN})]^+$ were fixed to the optimized values obtained from refinement on the 2 mM analyte data set. ^d $k_{\text{rev}} = k_{\text{fwd}}/K_{\text{eq}}$.

References

1. King, R. B.; Cloyd, J. C.; Kapoor, P. N. *J. Chem. Soc., Perkin Trans. 1* **1973**, 2226-2229.
2. Meier, U. W.; Hollmann, F.; Thewalt, U.; Klinga, M.; Leskelä, M.; Rieger, B. *Organometallics* **2003**, *22*, 3905-3914.